

Studies of laser-plasma interaction physics with low-density targets for direct-drive inertial confinement schemes

Cite as: Matter Radiat. Extremes 4, 045402 (2019); doi: 10.1063/1.5090965

Submitted: 31 January 2019 • Accepted: 2 April 2019 •

Published Online: 31 May 2019



View Online



Export Citation



CrossMark

V. Tikhonchuk,^{1,2,a)} Y. J. Gu,^{1,3} O. Klimo,^{1,4} J. Limpouch,⁴ and S. Weber¹

AFFILIATIONS

¹ ELI-Beamlines, Institute of Physics, Academy of Sciences of the Czech Republic, 18221 Prague, Czech Republic

² Centre Lasers Intenses et Applications, University of Bordeaux–CNRS–CEA, Talence 33405, France

³ Institute of Plasma Physics of the CAS, Za Slovankou 1782/3, 18200 Prague, Czech Republic

⁴ FNSPE, Czech Technical University in Prague, 11519 Prague, Czech Republic

^{a)} Electronic mail: vladimir.tikhonchuk@eli-beams.eu.

ABSTRACT

Comprehensive understanding and possible control of parametric instabilities in the context of inertial confinement fusion (ICF) remains a challenging task. The details of the absorption processes and the detrimental effects of hot electrons on the implosion process require as much effort on the experimental side as on the theoretical and simulation side. This paper describes a proposal for experimental studies on nonlinear interaction of intense laser pulses with a high-temperature plasma under conditions corresponding to direct-drive ICF schemes. We propose to develop a platform for laser-plasma interaction studies based on foam targets. Parametric instabilities are sensitive to the bulk plasma temperature and the density scale length. Foam targets are sufficiently flexible to allow control of these parameters. However, investigations conducted on small laser facilities cannot be extrapolated in a reliable way to real fusion conditions. It is therefore necessary to perform experiments at a multi-kilojoule energy level on medium-scale facilities such as OMEGA or SG-III. An example of two-plasmon decay instability excited in the interaction of two laser beams is considered.

© 2019 Author(s). All article content, except where otherwise noted, is licensed under a Creative Commons Attribution (CC BY) license (<http://creativecommons.org/licenses/by/4.0/>). <https://doi.org/10.1063/1.5090965>

I. INTRODUCTION

The physics of laser-plasma interaction is an indispensable part of research in inertial confinement fusion (ICF). It defines the efficiency of laser energy transfer to the target, the quality and quantity of laser energy absorption, and such undesirable processes as hard x-ray and hot-electron generation. It is, however, difficult to scale up laser-plasma experiments performed on small-scale (sub-kilojoule) laser facilities where plasmas have smaller spatial scale and/or lower temperatures. For appropriate modeling of laser-plasma interaction in the coronas of fusion-relevant targets, one needs to create plasmas of spatial size 300–500 μm and with temperatures of 3–5 keV. The internal energy of such a hot plasma with density close to critical is of the order of a few kilojoules. There are a limited number of laser facilities that are able to provide access to the required parameters. The corresponding hot and dense plasmas can be created on the surface of a thick solid target,^{1–3} with spherical targets,⁴ or by using

low-density foams.⁵ The major questions that need to be addressed in laser-plasma interaction studies are related to scaling of the processes studied on smaller and colder plasmas to ignition-size targets at laser intensities exceeding 10^{15} W/cm² and at laser wavelengths varying from 0.5 to 0.35 μm . These questions are as follows: (i) How efficiently can one transport laser energy through a large low-density corona to the near-critical region? (ii) How large can the laser absorption be, and how can it be improved? (iii) What fraction of the absorbed laser energy is transferred to suprathermal electrons, and how can one control their number and energy? At present, there are no reliable methods for controlling the parametric instabilities, and there is a serious risk of adverse effects from these when conditions for ignition are attained. In this paper, we propose a platform for experimental studies of laser-plasma interactions for ICF ignition conditions. We include a choice of appropriate targets, diagnostics, and experimental setups.

The remainder of the paper is structured as follows. Section II describes in some detail the properties of foam targets. Section III describes the various interaction configurations to be considered. The single-beam scenario is considered in Sec. IV and the multiple-beam scenario in Sec. V. Finally, conclusions are presented in Sec. VI.

II. TARGETS

Spherical irradiation geometries are available only on the OMEGA and GEKKO-XII facilities, but the available laser energy is too small (30 and 3 kJ, respectively) to attain the required plasma parameters. Therefore, we discuss here possible experiments in a planar geometry using either solid or foam targets. Solid targets offer the possibility of creating a planar expanding plasma with density scale length exceeding $100\ \mu\text{m}$ and expanding with supersonic velocity. Typically, two sets of laser beams are needed. The first set of beams, called the prepulse, serves to create an expanding plasma. By varying the delay between the prepulse and the main pulse, one can vary the plasma density scale length. The prepulse needs to be focused on a large spot of diameter $500\text{--}800\ \mu\text{m}$ and to be sufficiently energetic to maintain a sufficiently high plasma temperature. Typically, such a setup requires energies of the order of a few kilojoules or more.^{1,3}

The advantage of solid targets is the possibility of combining measurements of absorption and reflection with measurements of energy transferred to the target and to hot electrons. For this, the targets typically contain multiple layers behind the ablator that allow measurement of hot-electron number and energy and of ablation and shock-wave pressure.⁶ With these targets, it is easy to achieve supersonic plasma expansion velocities, which are important for studying effects such as beam bending and cross-beam energy transfer (CBET).

Typically, these targets consist of several layers made of different materials. The first layer—the ablator, made of plastic—serves for plasma production and interaction studies, one or two metallic layers behind it serve for hot-electron measurements, and the final layer, made of plastic or quartz, serves for shock measurements. Hot electrons entering the metallic layers produce characteristic $K\alpha$ emission, with the number of photons being proportional to the number of electrons with energies above the K-edge cutoff.⁷ By comparing the number of x-ray photons emitted from two different metallic layers, one can estimate also a characteristic hot-electron temperature. This can also be measured from bremsstrahlung emission of hot electrons in the ablator. The shock pressure is estimated either by measuring the time needed for the shock to propagate through the transport layer with pyrometry⁸ or by measuring the shock velocity with interferometry.⁹

Low-density foams are frequently used as targets for laser-plasma interaction experiments because they can be easily converted into large-volume homogeneous plasmas, which are of interest in many applications, such as ICF, bright x-ray sources, and studies of material properties under extreme conditions. The major advantage of foam targets is their rapid conversion from a structured solid material into a quasi-homogeneous plasma under intense radiation, with a flow velocity gradient that can be controlled by the foam thickness and the time delay between the heating and interaction laser pulses. The temperature of this plasma can be varied by choosing the laser intensity and wavelength.

There have been a number of developments in foam technology during the last 10–15 years.¹⁰ Plastic foams with density varying from 2 to $30\ \text{mg}/\text{cm}^3$ and of millimeter size can be created and supported in a metallic holder. These foam targets are fairly reproducible, with pore size of the order of $1\text{--}2\ \mu\text{m}$, and their chemical composition can be varied by mixing different elements. They are quickly homogenized under the action of intense laser or x-ray radiation.

There are two possibilities for foam ionization in experiments. The foam is ionized either by a flash of x-ray emission from a thin metallic layer covering the foam or by preforming laser beams, producing a plasma with the required density and temperature. The x-ray flash is a convenient approach, since the foam is transparent to radiation and the created plasma is rather homogeneous. However, because of the small optical depth of the plasma, its temperature is quite low. For example, according to Ref. 11, foams of density $5\text{--}20\ \text{mg}/\text{cm}^3$ ionized by copper x-rays produced with a 60 J, 600 ps laser pulse gave a plasma temperature of less than 10 eV. Another possibility is foam ionization with a laser-sustained supersonic ionization wave. For laser pulse intensity in the range $10^{14}\text{--}10^{15}\ \text{W}/\text{cm}^2$, the ionization front velocity is $400\text{--}700\ \text{km}/\text{s}$, and a plasma of thickness of $\sim 500\ \mu\text{m}$ can be created with a pulse duration of approximately 1 ns.^{5,12} A theoretical model describing propagation of an ionization wave in foam has been developed in Refs. 13–15. One can estimate qualitatively the laser energy needed for plasma formation. As a figure of merit, we consider a $10\ \text{mg}/\text{cm}^3$ foam of diameter 1 mm and thickness 1 mm. The volume of the foam is $\sim 1\ \text{mm}^3$ and it has mass $10\ \mu\text{g}$. To fully ionize and heat such a plasma to a temperature of 1 keV, one needs to provide an energy of 100 MJ/g. Assuming an energy deposition efficiency of 50%, one would need an energy of $\sim 10\ \text{kJ}$ to raise the temperature to a level of 3–5 keV. This example illustrates the need for a large-scale facility.

A photograph of a typical foam target is shown in Fig. 1. The foam has the form of a disk of diameter 1–2 mm and thickness $200\text{--}800\ \mu\text{m}$. It is supported by a metallic washer of the same thickness with a transverse slot for observation of x-ray emission from the ionization front. The plasmas created from foams are rather homogeneous, with a characteristic spatial scale of the order of the foam thickness. They are also rather easily accessible for optical and x-ray diagnostics, but there is a problem with the detection of hot electrons,

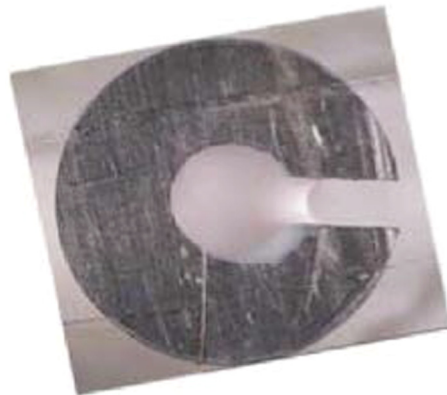


FIG. 1. Photograph of a foam target inserted in a washer. The foam diameter is 2 mm. Reprinted with permission from Depierreux *et al.*, *Phys. Rev. Lett.* **102**, 195005 (2009). Copyright 2009 by the American Physical Society.¹²

although these can be detected, and their effective temperature measured, by doping the foam with a high- Z element and measuring characteristic $K\alpha$ and/or bremsstrahlung emission. Another possibility would be to detect the electrons escaping the target. However, none of these methods will provide a quantitative value for the total number of hot electrons. This problem requires special attention.

III. POSSIBLE INTERACTION GEOMETRIES AND CORRESPONDING PARAMETERS

Modeling of plasma formation and design of the interaction geometry allowing formation of a large-size homogeneous plasma on high-energy laser installations such as SG-III Prototype and SG-III is the first goal of this project. Based on the expected plasma characteristics, a variety of original experiments can be planned. We demonstrate here several experimental setups that could be interesting for testing the features of parametric instabilities under conditions relevant to ICF in direct- or indirect-drive geometries. The experimental design is based on the actual performance of the SG-III Prototype.¹⁶ The laser facility has eight beams operating at a wavelength of 351 nm and equipped with continuous-phase plates. Each beam delivers an energy of up to 1 kJ in a 1–3 ns pulse with a controlled temporal profile. The focal-spot diameter can be varied from 0.5 to 2 mm, and the maximum intensity of a single beam in the focal spot can be $\sim 10^{15}$ W/cm². The beams are evenly distributed over cones of 45° and 135° with respect to the chamber axis. Thus, a group of four beams can be focused in a large focal spot of diameter ~ 1 mm and used for performing a plasma with desired parameters.

The other four beams can be used as interaction beams or as sources for x-ray radiography. The intensity domain of interest for the interaction beams is in the range of 10^{15} – 10^{16} W/cm², which cannot be achieved with currently available phase plates. It is therefore desirable for laser-plasma interaction experiments to equip one or two laser beams with smaller phase plates capable of focusing the beams in a 100 μ m diameter spot. With such a development, the whole intensity domain of interest could be scanned. It is also desirable to implement temporal smoothing techniques and controlled spectral broadening, at least for the interaction beams. That would allow such important problems as control of parametric instabilities to be addressed. The installation also provides one high-power (PW) beam that can be used for proton radiography of laser-driven shocks and self-generated electric and magnetic fields.

IV. SINGLE-BEAM INTERACTION

Propagation of a single interaction beam in a prepared plasma is of principal importance for designing schemes with efficient laser absorption and low-level scattering from an underdense plasma. There is a problem with controlling the level of stimulated Raman scattering (SRS), which in some experiments can attain $\sim 50\%$, accompanied by significant numbers of hot electrons. There are two qualitatively different explanations for such a strong SRS. One is related to SRS saturation by the secondary Langmuir decay instability (LDI). This process involves secondary ion-acoustic waves, in which the dissipation is controlled by the charge-to-mass ratio of ion species in the plasma.^{17,18} It was demonstrated experimentally that by adding heavier ion species to a plasma, one can decrease ion-acoustic wave damping, decrease the LDI threshold, and thus saturate the SRS at a lower level.^{19,20} This observation was confirmed in a more recent

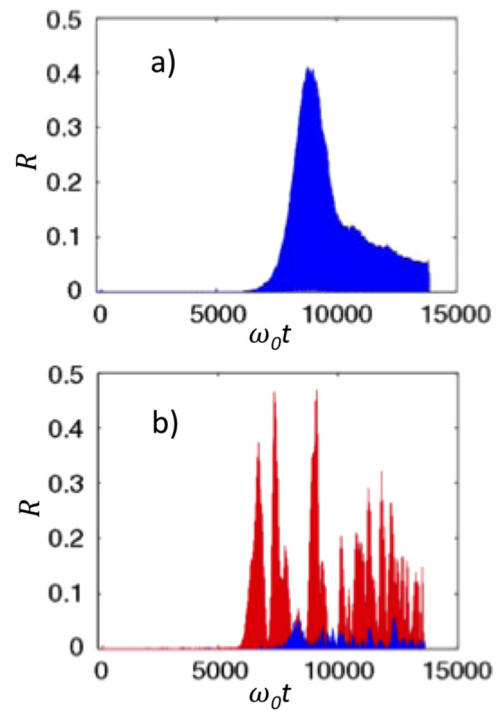


FIG. 2. Characteristic temporal evolution of backscattered emission in the SRS (blue) and SRS (red) wavelength domains for the case of laser interaction with plasmas of temperature 2 keV (a) and 10 keV (b). The laser intensity is $\sim 10^{16}$ nm. Reprinted with permission from Weber and Riconda, *High Power Laser Sci. Eng.* **3**, e6 (2015). Copyright Authors 2015, licensed under a Creative Commons Attribution License.²³

experiment,⁴ where a high level of SRS and hot-electron production was reported only in plastic targets containing hydrogen and where the ion-acoustic damping was assumed to be relatively high.

Another regime of SRS evolution has been found in hot and low-density plasmas, where daughter plasma waves are suppressed owing to strong Landau damping. It was demonstrated experimentally^{21,22} that the SRS reflectivity increases with time because of gradual suppression of Landau damping due to electron trapping in a growing plasma wave. Such an inflationary SRS is expected to operate in hot plasma and may generate less-energetic electrons. However, a transition from the LDI saturation regime to the inflationary regime has not been studied experimentally. It is expected to occur in plasmas with temperatures of a few kiloelectron volts and could be of great importance for ignition-scale targets. Moreover, in the same electron temperature range of a few kiloelectron volts, there is competition between SRS and the two-plasmon decay (TPD) instability that develops near quarter critical density and manifests itself in hot-electron generation. TPD is expected to dominate at relatively low plasma temperatures of 1–3 keV, while SRS is expected to be more important at higher temperatures.^{3,23} Direct experimental demonstration of such competition is still pending, despite its importance for ICF studies.

Competition between SRS and TPD and between the LDI and inflationary saturation regimes can be studied in foam-produced plasmas where the density, temperature, and species content can be controlled independently. Identification of the dominant parametric

instability (SRS or TPD) and the dominant saturation regime (LDI or inflation) can be performed by analyzing the frequency spectrum and angular distribution of the scattered radiation and the energy and angular distribution of hot electrons. An example of the temporal evolution of the laser reflected light is presented in Fig. 2 for two cases differing in plasma temperature. In the case of a low plasma temperature in Fig. 2(a), the TPD and stimulated Brillouin scattering (SBS) instabilities dominate, and the reflected light is weakly shifted in wavelength (less than 10% of the main wavelength). In contrast, in the hot plasma [Fig. 2(b)], SRS dominates the plasma response, and the backscattered light is strongly downshifted (marked in red in the figure).

There is additional interest in single-beam interaction studies in relation to SRS. Its growth rate depends directly on ion-acoustic damping and should exhibit anticorrelation with SRS in the LDI regime. It is expected²⁴ that adding light-hydrogen ions to a plasma will increase ion-acoustic wave damping and suppress SRS, while it will also suppress LDI and thus promote SRS to a higher level. Another possibility is spectral broadening of the laser beam. About 0.1% spectral width could be sufficient for significant SRS suppression. However, a spectral width an order of magnitude larger would be needed for SRS control. The scheme described above is, however, a simplified vision of the competition process. A speckled structure of the incident laser beam, self-focusing, and refraction may significantly alter the plasma response.²⁵

V. EXCITATION OF PARAMETRIC INSTABILITIES IN THE FIELD OF MULTIPLE BEAMS

Multibeam laser-plasma interaction is an indispensable part of any ICF scheme. In the direct-drive scheme, the focal spots of different laser beams overlap over the target surface to produce target irradiation that is as homogeneous as possible. Interaction of incident and reflected laser beams gives rise to cross-beam energy transfer (CBET),^{26,27} double stimulated scattering where both laser beams excite a common plasma or ion-acoustic wave,²⁸ and multibeam TPD.^{29–31} In the indirect-drive scheme, the laser beams cross each other in the laser entrance hole, exciting collective parametric instabilities.³² The consequences of these multibeam interactions are not sufficiently understood at present.

A. Cross-beam interaction

The CBET process corresponds to energy exchange between two electromagnetic waves via a common ion-acoustic wave. This is a version of SRS where both pump and seed waves have comparable amplitudes and frequencies, while the resonance ion-acoustic wave is excited locally owing to the Doppler frequency shift of the interference pattern of the waves in the flow of the expanding plasma. As the energy is transferred to the lower-frequency wave, it is the outgoing wave that picks up energy from the ingoing one.

That process induces undesirable energy losses and absorption asymmetry. It accounts for 30%–40% of the energy losses in the polar direct drive scheme on the OMEGA-scale targets.³³ One possibility that can be tested is to dope the ablator with lighter ion species, which will increase ion-acoustic damping and decrease CBET efficiency.²⁴ Another possibility is to use spectrally broadened laser beams. The most common method for modeling CBET is based on ray tracing³⁴ and paraxial complex geometrical optics.³⁵ More detailed simulations with electromagnetic codes have been developed recently.^{36,37} In contrast to simpler

methods for CBET modeling, they will allow the design of experiments under controllable conditions. In particular, it has been predicted that self-focusing of speckled beams may significantly increase the transferred power and may stimulate SRS in the direction common to both interacting beams. An example of such energy exchange ratio dependence on the intensity ratio of the incident beams is shown in Fig. 3.

These issues need to be investigated further, in particular in the context of their potential contribution to the rapidly expanding domain of plasma optics, i.e., the manipulation of high-intensity laser beams with plasmas.^{38,39} Future developments of CBET involving short-pulse laser beams could be a promising method of plasma-optical parametric amplification⁴⁰ that could be upscaled to a kilojoule level.

B. Excitation of parametric instabilities in the field of two laser beams

When two or more laser beams overlap in a plasma, excitation of SRS and TPD can be enhanced in special directions corresponding to resonant interaction of both laser beams with a common daughter wave. In the context of TPD, such processes have been studied theoretically by Myatt *et al.*³⁰ and experimentally at the OMEGA facility at laser intensities below 10^{15} W/cm² and plasma temperatures less than 1 keV.³¹ Excitation of SRS in the direction bisecting two laser beams has been reported in Ref. 5. It was demonstrated that such a double SRS may be responsible for strong scattering in some specific directions, although this may not be detectable with currently available diagnostics. Moreover, it may be related to excitation of strong plasma waves and electron acceleration in some particular directions.⁴¹ Further studies of such multibeam laser parametric processes and their correlation with hot-electron production are of prime interest for ICF.

Studies of CBET and parametric instabilities with two crossing beams can be conducted in a similar experimental setup. The difference lies in the orientation of the beam with respect to the plasma flow and the detection directions. In the case of CBET, the plasma flow is transonic

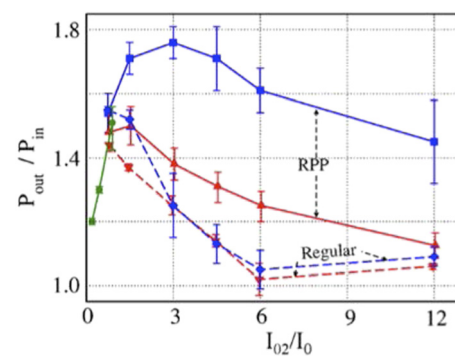


FIG. 3. Dependence of the power amplification of the second (receptor) beam on its intensity normalized to the reference intensity $I_0 = 9 \times 10^{14}$ W/cm². The incident beams have the same intensity. The solid lines show the energy exchange of two speckled beams with and without account being taken of speckle self-focusing (blue and red, respectively). The dashed lines show similar predictions for regular Gaussian beams. Reprinted with permission from Raj and Hüller, Phys. Rev. Lett. **118**, 055002 (2017). Copyright 2017 by the American Physical Society.³⁶

and has to be directed perpendicularly to the common direction of both beams. The energy is expected to be transmitted in the direction of the wave propagating downstream with respect to the flow. The efficiency of energy exchange can be controlled by the plasma flow velocity, the ratio of light to heavy ion species, the angle of beam crossing, and the spatial and temporal smoothing. Foam targets can be especially useful for studies of transonic flows, because the velocity gradient can be independently controlled.

A representative case of competition of parametric instabilities driven by multiple beams is the competition between TPD and SRS in an inhomogeneous plasma in the field of two laser beams of equal intensities and p-polarization incident at angles $\pm\theta$ with respect to the density gradient. The maximum growth rate of the TPD instability is $\gamma_{\text{TPD}} \approx \frac{1}{4} k_0 c a_0$, where $k_0 = (\sqrt{3}/2) \omega_0/c$ is the laser wavenumber at quarter critical density, $a_0 = eE_0/m_e \omega_0 c$ is the dimensionless laser amplitude, and ω_0 is the laser frequency. This instability corresponds to excitation of two plasma waves with wavenumber components parallel (k_{\parallel}) and perpendicular (k_{\perp}) to the laser propagation direction that are related by

$$k_{\parallel} = \frac{1}{2} k_0 \pm \sqrt{\frac{1}{4} k_0^2 + k_{\perp}^2}. \quad (1)$$

The common plasma wave can be found at the intersection of the resonance curves corresponding to the two laser waves. An example of such a resonance configuration is shown in Fig. 4(a). The common plasma wave (green) propagates in the direction bisecting two laser waves (black). Its wavenumber $k_{p1} = k_0 \cos \theta / \cos 2\theta$. The plasma waves excited in this configuration (k_{p1} , k_{p2} , and k'_{p2}) have a growth rate twice that of the standard TPD. It is expected that hot electrons will be generated preferentially in the direction of the common plasma wave. The angle 2θ between the laser beams controls the phase velocity of this wave,

$$v_{\text{ph1}} = \frac{c}{\sqrt{3}} \frac{\cos 2\theta}{\cos \theta}, \quad (2)$$

and thus the hot-electron energy. This phase velocity decreases as the angle between the laser beams increases, and this double TPD is suppressed for angles θ larger than $\sim 40^\circ$.

Excitation of SRS with two laser beams may proceed with either common scattered waves [Fig. 4(b)] or common plasma waves [Fig. 4(c)] for both forward and backward scattering. Resonance with a common plasma wave can be realized only under the condition $(\omega_0/c) \sin \theta_0 \leq k_s$, which limits the range of plasma densities to $n_e \leq n_s$, with

$$\frac{n_s}{n_c} = \frac{\cos^2 \theta_0}{1 + \sqrt{\cos^4 \theta_0 + \sin^2 \theta_0}}, \quad (3)$$

where θ_0 is the angle of laser incidence on the plasma. The electron density n_s corresponds to the particular situation where the common scattered wave propagates perpendicularly to the density gradient (assuming that the laser waves propagate symmetrically with respect to the density gradient). In that configuration, the SRS threshold is very low and is probably the first to be excited. The common plasma waves propagate in the direction of bisection, and their phase velocity can also be controlled by the angle between the laser beams. Configurations similar to those shown in Figs. 4(b) and 4(c) can also be realized for the SRS process.

C. Kinetic simulation of the two-laser-beam interaction

To evaluate nonlinear effects in the interaction of two laser beams with an inhomogeneous plasma, a series of kinetic simulations are performed with the particle-in-cell (PIC) code EPOCH⁴² in a planar two-dimensional geometry. We present here a generic setup where two laser beams of equal intensity $I_0 = 8 \times 10^{14}$ W/cm² at a wavelength $\lambda = 350$ nm enter a box $400\lambda \times 320\lambda$ from the left at angles $\theta_0 = \pm 20^\circ$ with respect to the normal (x axis). Both beams are p-polarized and have a flat-top intensity profile of width $\sim 50\lambda$. The intensity increases with time during the first 850 laser periods and then remains constant. The full simulation time is about 7.5 ps, which is sufficient to attain a quasistationary regime of interaction. Open boundary conditions are applied to the fields.

As we are interested in exploring the interaction processes near quarter critical density for ignition-size targets, the plasma temperature is set to $T_e = 3$ keV for electrons, and a low ion temperature $T_i = 170$ eV is chosen to ensure weak ion-acoustic wave damping. We consider a CH plasma with effective ion charge $Z = 3.5$ and effective

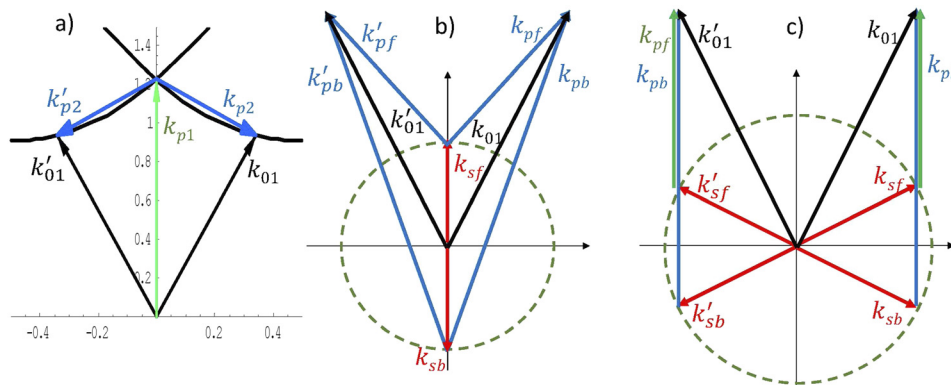


FIG. 4. Scheme of resonance interactions for TPD (a) and SRS [(b) and (c)] excited by two laser waves with wavenumbers k_{01} and k'_{01} propagating at angles $\pm\theta$ with respect to the density gradient. The axes are in units of ω_0/c . (a) and (c) show the interactions with common plasma waves (green and blue), and (b) shows the interactions with common scattered waves (red).

atomic mass $A = 6.5$. The plasma density varies linearly from $0.01n_c$ to $0.3n_c$ over a length of 345λ . Absorbing boundary conditions are applied to the particles. A mesh resolution $\delta x = \delta y = 0.02\lambda$ and a time step $\delta t = 0.08 \omega_0^{-1}$ are chosen to resolve the Debye length. Eight particles per cell, 4 ions and 4 electrons, were used in that simulation. The physical parameters are rather similar to those considered in Ref. 30, except that we do not account for electron collisions, but our density profile is extended to lower densities, thus allowing account to be taken also of the SRS and SBS processes.

Numerical simulations show that the TPD instability dominates under the conditions considered here. The threshold intensity of the standard TPD³⁰ is $5.8 \times 10^{14} \text{ W/cm}^2$. This is lower than the intensity of each beam, the plasma waves are excited on a time scale of a few picoseconds, and their level remains approximately constant throughout the simulation time, with the effective electric field amplitude attaining high values of $eE_x \sim 0.1m_e\omega_0c$ and remaining localized in a narrow zone of about 10 laser wavelengths near quarter critical density. This value of the electric field is about 10 times larger than the value reported in Ref. 30, indicating that the approach based on solving the Zakharov equations might be inappropriate in the case considered here.

The physical processes occurring in laser-plasma interaction can be characterized by considering the Fourier spectra of the electromagnetic and plasma waves shown in Fig. 5. The bright spot in Fig. 5(a) represents the incident laser waves. As their wave vectors have x components that are equal and y components that are of opposite sign, they are represented by a single point at $k_x = 0.80\omega_0/c$ and $k_y = 0.34\omega_0/c$. A narrow bright point at $k_x = 0, k_y = 0.68\omega_0/c$ in the ion density spectrum in Fig. 5(c) corresponds to interference of two pump waves.

The bright circle with wavenumber $k \approx 0.9\omega_0/c$ in Fig. 5(a) represents the SBS waves originating from plasma densities comparable to or larger than $n_c/4$. The scattered waves propagate in directions nearly opposite to the pump directions. They correspond to double SBS on the common ion-acoustic wave having wave vector components $k_x \approx 1.6\omega_0/c$ and $k_y = 0$, with the scattered waves propagating in the directions opposite to the pump waves.

The double TPD instability can be clearly seen in the spectrum of charge fluctuations in Fig. 5(b), representing essentially electron plasma waves. The common plasma wave, according to Eq. (1), has wave vector $k_x = 1.16 \omega_0/c$ and $k_y = 0$. This wave is the dominant feature in the charge density spectrum in Fig. 5(b). A second plasma wave with wave vector $k_x = -0.36\omega_0/c$ and $k_y = 0.34\omega_0/c$ is also clearly seen in the spectrum, but with a smaller amplitude. The resonantly driven plasma wave undergoes secondary modulation instability, leading to a spread in its angular spectrum.

Excitation of the common plasma wave presents a convenient way to control hot-electron acceleration and energy transport. According to Eq. (2), the phase velocity of the common wave in the case considered here is $0.43c$, corresponding to a resonant electron energy of 56 keV. The characteristic velocity of an electron trapped in this plasma wave, $v_{tr} = (eE_x/m_e k_p)^{1/2} \approx 0.3c$, is comparable to the phase velocity. One may therefore expect accelerated electrons in the energy range 40–100 keV. Indeed, Fig. 6(a) shows that a tail in the electron energy distribution appears at an energy of ~ 30 keV and extends to 150 keV, with a characteristic exponential slope corresponding to an effective temperature of 15 keV. Such a steep energy slope is a result of a relatively narrow spectrum and high amplitude of

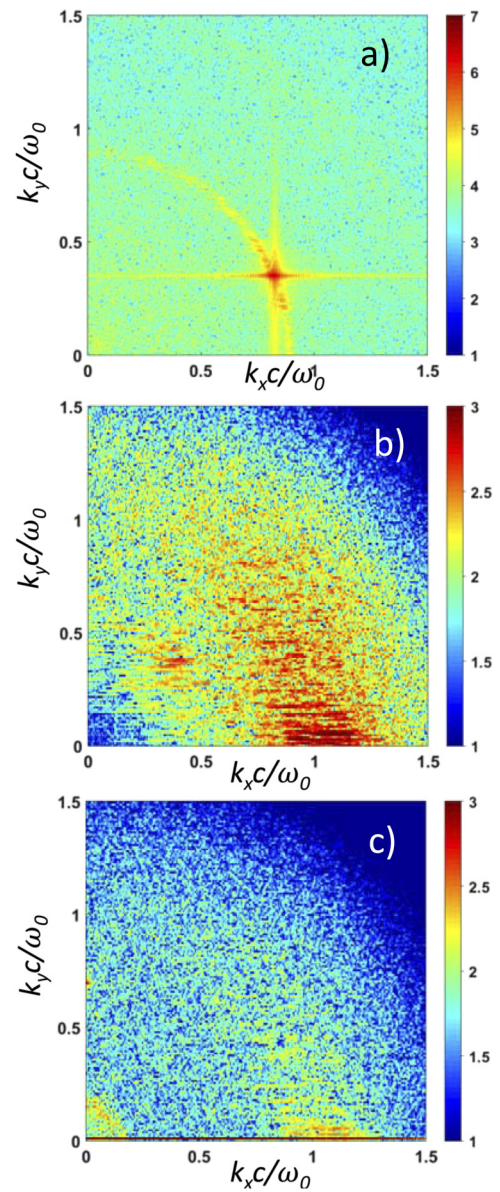


FIG. 5. Spectra (in logarithmic units) of the magnetic field B_z (a), charge density $n_i - n_e$ (b), and ion density n_i (c) calculated at time $t = 7.5$ ps. The instantaneous spectra do not resolve the sign of the wave vectors, so only a quarter of the Fourier space corresponding to absolute values of k_x and k_y is shown. The simulation parameters are presented in the text.

the plasma wave, which is located near the resonant wavenumber [see Fig. 5(b)] with an angular spread. Correspondingly, the electrons are accelerated in a relatively broad opening angle of $\sim 30^\circ$ in the forward direction [see Fig. 6(b)]. The possibility of controlling the energy spectrum of accelerated electrons by changing the angle between the pump waves merits experimental confirmation. Competition of the double TPD with SBS and SRS instabilities is also a potential subject for experimental investigation.

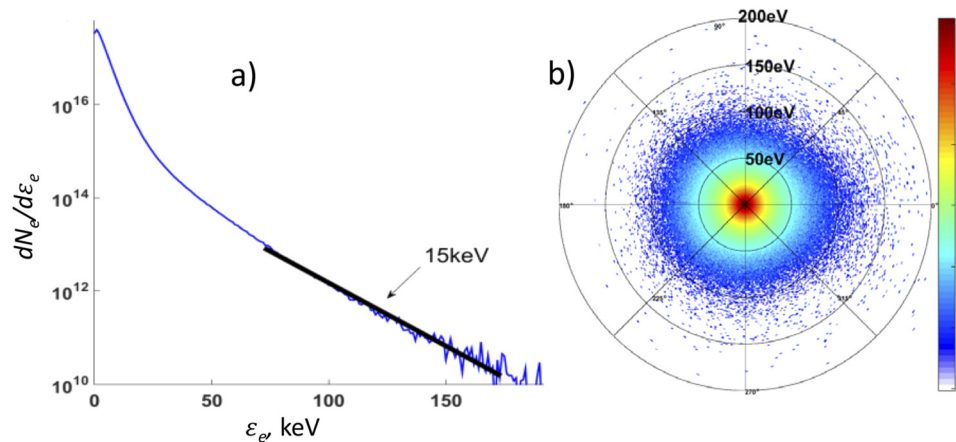


FIG. 6. Energy distribution of electrons in the interaction region near quarter critical density (a) and their angular distribution (b). The simulation parameters are the same as in Fig. 5.

The overall efficiency of laser absorption due to the TPD process is relatively modest in the example considered here. We observe about 5% of the incident laser flux scattered in the backward direction, while 15%–20% is side-scattered and 65%–70% transmitted. The absorbed fraction of 5% is transmitted to hot electrons, which are accelerated near quarter critical density and carry the energy flux in the forward direction. That energy balance is qualitatively consistent with numerical simulations conducted using the Zakharov equations for plasma waves with one⁴³ and two³⁰ pump waves. However, the effective temperature of the hot electrons is lower in our case, while the absorbed energy flux is twice as great.

VI. CONCLUSIONS

The proposed studies of parametric instabilities cannot be accomplished in a single experimental campaign and require joint dedicated efforts over an extended period. This analysis provides a general perspective and demonstrates the importance of an experimental platform dedicated to laser-plasma interaction physics. The ELI-Beamlines group possesses numerical tools for design both of targets and of particular experiments. A single laser beam interaction for the conditions relevant to a shock ignition scheme is presented in Ref. 25. The basic target design can be performed using a radiation hydrodynamic code with a special module accounting for foam plasma homogenization in front of the ionization wave¹⁵ and for magnetic field generation. Laser-plasma interaction experiments can be designed with a hybrid approach combining hydrodynamic and kinetic simulations with a PIC code in two and possibly three spatial dimensions.

ACKNOWLEDGMENTS

The authors acknowledge support from the European Regional Development Fund for the following projects: HiFi (No. CZ.02.1.01/0.0/0.0/15_003/0000449), CAAS (No. CZ.02.1.01/0.0/0.0/16_019/0000778), ADONIS (No. CZ.02.1.01/0.0/0.0/16_019/0000789), and ELITAS (No. CZ.02.1.01/0.0/0.0/16_013/0001793). This work has received funding from the European Union Horizon 2020 Research and Innovation Programme under Grant Agreement No. 633053 (EUROfusion Project No. CfP-AWP17-IFE-CEA-01). Computational resources were provided by the MetaCentrum under the LM2010005

project, by the IT4Innovations Centre of Excellence under the CZ.1.05/1.1.00/02.0070 and LM2011033 projects, and by the ECLIPSE cluster of ELI-Beamlines. The EPOCH code was developed as part of the UK EPSRC-funded EP/G054940/1 project.

REFERENCES

- M. Hohenberger, W. Theobald, S. X. Hu, K. S. Anderson, R. Betti, T. R. Boehly, A. Casner, D. E. Fratanduono, M. Lafon, D. D. Meyerhofer, R. Nora, X. Ribeyre, T. C. Sangster, G. Schurtz, W. Seka, C. Stoeckl, and B. Yaakobi, "Shock-ignition experiments with planar targets on OMEGA," *Phys. Plasmas* **21**, 022702 (2014).
- G. Cristoforetti, L. Antonelli, S. Atzeni, F. Baffigi, F. Barbatto, D. Batani, G. Boutoux, A. Colaitis, J. Dostal, R. Dudzak, L. Juha, P. Koester, A. Marocchino, D. Mancelli, Ph. Nicolai, O. Renner, J. J. Santos, A. Schiavi, M. M. Skoric, M. Smid, P. Straka, and L. A. Gizzi, "Measurements of parametric instabilities at laser intensities relevant to strong shock generation," *Phys. Plasmas* **25**, 012702 (2017).
- M. J. Rosenberg, A. A. Solodov, J. F. Myatt, W. Seka, P. Michel, M. Hohenberger, R. Short, R. Epstein, S. P. Regan, E. M. Campbell, T. Chapman, C. Goyon, J. E. Ralph, M. A. Barrios, J. D. Moody, and J. W. Bates, "Origins and scaling of hot-electron preheat in ignition-scale direct-drive inertial confinement fusion experiments," *Phys. Rev. Lett.* **120**, 055001 (2018).
- W. Theobald, A. Bose, R. Yan, R. Betti, M. Lafon, D. Mangino, A. R. Christopherson, C. Stoeckl, W. Seka, W. Shang, D. T. Michel, C. Ren, R. C. Nora, A. Casner, J. Peebles, F. N. Beg, X. Ribeyre, E. Llor Aisa, A. Colaitis, V. Tikhonchuk, and M. S. Wei, "Enhanced hot-electron production and strong-shock generation in hydrogen-rich ablaters for shock ignition," *Phys. Plasmas* **24**, 120702 (2017).
- S. Depierreux, C. Neuville, C. Baccou, V. Tassin, M. Casanova, P.-E. Masson-Laborde, N. Borisenko, A. Orekhov, A. Colaitis, A. Debayle, G. Duchateau, A. Heron, S. Hüller, P. Loiseau, P. Nicolai, D. Pesme, C. Riconda, G. Tran, R. Bahr, J. Katz, C. Stoeckl, W. Seka, V. Tikhonchuk, and C. Labaune, "Experimental investigation of the collective Raman scattering of multiple laser beams in inhomogeneous plasmas," *Phys. Rev. Lett.* **117**, 235002 (2016).
- D. Batani, L. Antonelli, F. Barbatto, G. Boutoux, A. Colaitis, J.-L. Feugeas, G. Folpini, D. Mancelli, Ph. Nicolai, J. J. Santos, J. Trela, V. Tikhonchuk, J. Badziak, T. Chodukowski, K. Jakubowska, Z. Kalinowska, T. Pisarczyk, M. Rosinski, M. Sawicka, F. Baffigi, G. Cristoforetti, F. D. Amato, P. Koester, L. A. Gizzi, S. Viciani, S. Atzeni, A. Scavi, M. Skoric, S. Gus'kov, J. Honrubia, J. Limpouch, O. Klimo, J. Skala, Y. J. Gu, E. Krousky, O. Renner, M. Smid, S. Weber, R. Dudzak, M. Krus, and J. Ullschmied, "Progress in understanding the role of hot electrons for the shock ignition approach to inertial confinement fusion," *Nucl. Fusion* **59**, 032012 (2019).
- T. Hall, S. Ellwi, D. Batani, A. Bernardinello, V. Masella, M. Koenig, A. Benuzzi, J. Krishnan, F. Pisani, A. Djaou, P. Norreys, D. Neely, S. Rose, M. Key, and P. Fews, "Fast

- electron deposition in laser shock compressed plastic targets," *Phys. Rev. Lett.* **81**, 1003 (1998).
- ⁸J. E. Miller, T. R. Boehly, A. Melchior, D. D. Meyerhofer, P. M. Celliers, J. H. Eggert, D. G. Hicks, C. M. Sorce, J. A. Oertel, and P. M. Emmel, "Streaked optical pyrometer system for laser-driven shock-wave experiments on OMEGA," *Rev. Sci. Instrum.* **78**, 034903 (2007).
- ⁹P. M. Celliers, G. W. Collins, D. K. Bradley, S. J. Moon, D. H. Munro, R. Cauble, D. M. Gold, L. B. D. Silva, F. A. Weber, R. J. Wallace, B. A. Hammel, and W. W. Hsing, "Visar for measuring equation of state and shock propagation in liquid deuterium," *Rev. Sci. Instrum.* **72**, 1038 (2001).
- ¹⁰K. Nagai, C. S. A. Musgrave, and W. Nazarov, "A review of low density porous materials used in laser plasma experiments," *Phys. Plasmas* **25**, 030501 (2018).
- ¹¹S. N. Chen, T. Iwawaki, K. Morita, P. Antici, S. D. Baton, F. Filippi, H. Habara, M. Nakatsutsumi, Ph. Nicolai, W. Nazarov, C. Rousseaux, M. Starodubstev, K. A. Tanaka, and J. Fuchs, "Density and temperature characterization of long-scale length, near-critical density controlled plasma produced from ultra-low density plastic foam," *Sci. Rep.* **6**, 21495 (2017).
- ¹²S. Depierreux, C. Labaune, D. T. Michel, C. Stenz, Ph. Nicolai, M. Grech, G. Riazuelo, S. Weber, C. Riconda, V. T. Tikhonchuk, P. Loiseau, N. G. Borisenko, W. Nazarov, S. Hüller, D. Pesme, M. Casanova, J. Limpouch, C. Meyer, P. Di-Nicola, R. Wrobel, E. Alozy, P. Romary, G. Thiell, G. Soullie, C. Reverdin, and B. Vilette, "Laser smoothing and imprint reduction with a foam layer in the multikilojoule regime," *Phys. Rev. Lett.* **102**, 195005 (2009).
- ¹³S. Y. Guskov, J. Limpouch, Ph. Nicolai, and V. T. Tikhonchuk, "Laser-supported ionization wave in under-dense gases and foams," *Phys. Plasmas* **18**, 103114 (2011).
- ¹⁴S. Yu. Gus'kov, M. Cipriani, R. De Angelis, F. Consoli, A. A. Rupasov, P. Andreoli, G. Cristofari, and G. Di Giorgio, "Absorption coefficient for nanosecond laser pulse in porous material," *Plasma Phys. Controlled Fusion* **57**, 125004 (2015).
- ¹⁵J. Velechovsky, J. Limpouch, R. Liska, and V. Tikhonchuk, "Hydrodynamic modeling of laser interaction with micro-structured targets," *Plasma Phys. Controlled Fusion* **58**, 095004 (2016).
- ¹⁶C. Tian, L. Shan, B. Zhang, W. Zhou, D. Liu, B. Bi, F. Zhang, W. Wang, B. Zhang, and Y. Gu, "Realization of high irradiation uniformity for direct drive ICF at the SG-III prototype laser facility," *Eur. Phys. J. D* **69**, 54 (2015).
- ¹⁷H. A. Rose, D. F. DuBois, and B. Bezzerides, "Nonlinear coupling of stimulated Raman and Brillouin scattering in laser-plasma interactions," *Phys. Rev. Lett.* **58**, 2547 (1987).
- ¹⁸T. Kolber, W. Rozmus, and V. T. Tikhonchuk, "Saturation of stimulated Raman scattering by Langmuir and ion-acoustic wave coupling," *Phys. Fluids B* **5**, 138 (1993).
- ¹⁹J. C. Fernandez, J. A. Cobble, B. H. Failor, D. F. DuBois, D. S. Montgomery, H. A. Rose, H. X. Vu, B. H. Wilde, M. D. Wilke, and R. E. Chrien, "Observed dependence of stimulated Raman scattering on ion-acoustic damping in hohlraum plasmas," *Phys. Rev. Lett.* **77**, 2702 (1996).
- ²⁰R. K. Kirkwood, B. J. MacGowan, D. S. Montgomery, B. B. Afeyan, W. L. Kruer, J. D. Moody, K. G. Estabrook, C. A. Back, S. H. Glenzer, M. A. Blain, E. A. Williams, R. L. Berger, and B. F. Lasinski, "Effect of ion-wave damping on stimulated Raman scattering in high-Z laser-produced plasmas," *Phys. Rev. Lett.* **77**, 2706 (1996).
- ²¹J. C. Fernandez, J. A. Cobble, D. S. Montgomery, M. D. Wilke, and B. B. Afeyan, "Observed insensitivity of stimulated Raman scattering on electron density," *Phys. Plasmas* **7**, 3743 (2000).
- ²²J. L. Kline, D. S. Montgomery, L. Yin, D. F. DuBois, B. J. Albright, B. Bezzerides, J. A. Cobble, E. S. Dodd, D. F. DuBois, J. C. Fernandez, R. P. Johnson, J. M. Kindel, and H. A. Rose, "Different $k\lambda_D$ regimes for nonlinear effects on Langmuir waves," *Phys. Plasmas* **13**, 055906 (2006).
- ²³S. Weber and C. Riconda, "Temperature dependence of parametric instabilities in the context of the shock-ignition approach to inertial confinement fusion," *High Power Laser Sci. Eng.* **3**, e6 (2015).
- ²⁴V. Yu. Bychenkov, W. Rozmus, and V. T. Tikhonchuk, "Ion acoustic waves in plasmas with light and heavy ions," *Phys. Rev. E* **51**, 1400 (1995).
- ²⁵Y. J. Gu, O. Klimo, Ph. Nicolai, S. Shekhanov, S. Weber, V. Tikhonchuk, "Collective absorption of laser radiation in plasma at sub-relativistic intensities," *High Power Laser Sci. Eng.* (submitted).
- ²⁶I. V. Igumenshchev, D. H. Edgell, V. N. Goncharov, J. A. Delettrez, A. V. Maximov, J. F. Myatt, W. Seka, A. Shvydsky, S. Skupsky, and C. Stoeckl, "Crossed-beam energy transfer in implosion experiments on OMEGA," *Phys. Plasmas* **17**, 122708 (2010).
- ²⁷V. V. Eliseev, W. Rozmus, V. T. Tikhonchuk, and C. E. Capjack, "Interaction of crossed laser beams with plasmas," *Phys. Plasmas* **3**, 2215 (1996).
- ²⁸A. A. Zozulya, V. P. Silin, and V. T. Tikhonchuk, "Double stimulated scattering—a novel view on the nonlinear parametric processes in plasma," *Phys. Lett. A* **99**, 224 (1983).
- ²⁹C. Stoeckl, R. E. Bahr, B. Yaakobi, W. Seka, S. P. Regan, R. S. Craxton, J. A. Delettrez, R. W. Short, J. Myatt, and A. V. Maximov, "Multibeam effects on fast-electron generation from two plasmon-decay instability," *Phys. Rev. Lett.* **90**, 235002 (2003).
- ³⁰J. F. Myatt, H. X. Vu, D. F. DuBois, D. A. Russell, J. Zhang, R. W. Short, and A. V. Maximov, "Mitigation of two-plasmon decay in direct-drive inertial confinement fusion through the manipulation of ion-acoustic and Langmuir wave damping," *Phys. Plasmas* **20**, 052705 (2013).
- ³¹R. K. Follett, J. F. Myatt, J. G. Shaw, D. T. Michel, A. A. Solodov, D. H. Edgell, B. Yaakobi, and D. H. Froula, "Simulations and measurements of hot-electron generation driven by the multibeam two-plasmon-decay instability," *Phys. Plasmas* **24**, 102134 (2017).
- ³²D. F. DuBois, B. Bezzerides, and H. A. Rose, "Collective parametric instabilities of many overlapping laser beams with finite bandwidth," *Phys. Fluids B* **4**, 241 (1992).
- ³³J. A. Marozas, M. Hohenberger, M. J. Rosenberg, D. Turnbull, T. J. B. Collins, P. B. Radha, P. McKenty, J. D. Zuegel, F. J. Marshall, S. P. Regan, T. C. Sangster, W. Seka, E. M. Campbell, V. N. Goncharov, M. Bowers, J.-M. G. Di-Nicola, G. Erbert, B. J. MacGowan, L. J. Pelz, and S. T. Yang, "First observation of cross-beam energy transfer mitigation for direct-drive inertial confinement fusion implosions using wavelength detuning at the National Ignition Facility," *Phys. Rev. Lett.* **120**, 085001 (2018).
- ³⁴I. V. Igumenshchev, W. Seka, D. H. Edgell, D. T. Michel, D. H. Froula, V. N. Goncharov, R. S. Craxton, L. Divol, R. Epstein, R. Follett, J. H. Kelly, T. Z. Kosc, A. V. Maximov, R. L. McCrory, D. D. Meyerhofer, P. Michel, J. F. Myatt, T. C. Sangster, A. Shvydsky, S. Skupsky, and C. Stoeckl, "Crossed-beam energy transfer in direct-drive implosions," *Phys. Plasmas* **19**, 056314 (2012).
- ³⁵A. Colaitis, X. Ribeyre, E. Le Bel, G. Duchateau, Ph. Nicolai, and V. Tikhonchuk, "Influence of laser induced hot electrons on the threshold for shock ignition of fusion reactions," *Phys. Plasmas* **23**, 072703 (2016).
- ³⁶G. Raj and S. Hüller, "Impact of laser beam speckle structure on crossed beam energy transfer via beam deflections and ponderomotive self-focusing," *Phys. Rev. Lett.* **118**, 055002 (2017).
- ³⁷J. F. Myatt, R. K. Follett, J. G. Shaw, D. H. Edgell, D. H. Froula, I. V. Igumenshchev, and V. N. Goncharov, "A wave-based model for cross-beam energy transfer in direct-drive inertial confinement fusion," *Phys. Plasmas* **24**, 056308 (2017).
- ³⁸D. Turnbull, C. Goyon, G. E. Kemp, B. B. Pollock, D. Mariscal, L. Divol, J. S. Ross, S. Patankar, J. D. Moody, and P. Michel, "Refractive index seen by a probe beam interacting with a laser-plasma system," *Phys. Rev. Lett.* **118**, 015001 (2017).
- ³⁹R. K. Kirkwood, D. P. Turnbull, T. Chapman, S. C. Wilks, M. D. Rosen, R. A. London, L. A. Pickworth, W. H. Dunlop, J. D. Moody, D. J. Strozzi, P. A. Michel, L. Divol, O. L. Landen, B. J. MacGowan, B. M. V. Wouterghem, K. B. Fournier, and B. E. Blue, "Plasma-based beam combiner for very high fluence and energy," *Nat. Phys.* **14**, 80 (2018).
- ⁴⁰L. Lancia, A. Giribono, L. Vassura, M. Chiramello, C. Riconda, S. Weber, A. Castan, A. Chatelain, A. Frank, T. Gangolf, M. N. Quinn, J. Fuchs, and J.-R. Marques, "Signatures of the self-similar regime of strongly coupled stimulated Brillouin scattering for efficient short laser pulse amplification," *Phys. Rev. Lett.* **116**, 075001 (2016).
- ⁴¹E. L. Dewald, F. Hartemann, P. Michel, J. Milovich, M. Hohenberger, A. Pak, O. L. Landen, L. Divol, H. F. Robey, O. A. Hurricane, T. Döppner, F. Albert, B. Bachmann, N. B. M. A. J. MacKinnon, D. Callahan, and M. J. Edwards, "Generation and beaming of early hot electrons onto the capsule in laser-driven ignition hohlraums," *Phys. Rev. Lett.* **116**, 075003 (2016).
- ⁴²T. Arber, K. Bennett, C. Brady, A. Lawrence-Douglas, M. Ramsay, N. Sircombe, P. Gillies, R. Evans, H. Schmitz, A. Bell, and C. Ridgers, "Contemporary particle-in-cell approach to laser-plasma modeling," *Plasma Phys. Controlled Fusion* **57**, 113001 (2015).
- ⁴³H. X. Vu, D. F. DuBois, J. F. Myatt, and D. A. Russell, "Mitigation of two-plasmon decay in direct-drive inertial confinement fusion through the manipulation of ion-acoustic and Langmuir wave damping," *Phys. Plasmas* **19**, 102703 (2012).